VOL. 5, NO. 9, SEPTEMBER 2010 ISSN 1819-6608
ARPN Journal of Engineering and Applied Sciences


www.arpnjournals.com

NUMERICAL SIMULATION OF FLUID FLOW IN ENCLOSED ROTATING FILTER AND DISK

Yazan Taamneh
Department of Mechanical Engineering, Tafila Technical University Tafila, Jordan
E-Mail: ytaamneh@yahoo.com

ABSTRACT

Computational fluid dynamics is used to investigate the behaviour of the fluid flow near rotating filter and disk surface in closed housing. The study focused on the laminar flow and wide gap region. A commercial finite volume package FLUENT was used to visualize the nature of the flow surrounding the rotating disk. The fluid is assumed to be Newtonian, incompressible, non-fouling and isothermal. It was found that the viscous drag coefficient on the rotating filter and disk surface is strongly governed by the Reynolds number. The rotating filter in a closed housing was found to produce high viscous drag (shear stress) compared to rotating disk. Increasing the rotation speed of the filter increase the static pressure inside the filter due to centrifugal force induced inside it. Therefore, a back pressure phenomenon may be raised. Viscous drag coefficient for the case of disk rotating in closed housing was found to be in good agreement with previous experimental results.

Keywords: CFD simulation, rotating filter, laminar flow, wide gap.

1. INTRODUCTION

The estimation of the torque due to skin friction on rotating disks is important because of its application in the calculation of losses in many different industrial machinery [1-4]. The pioneering work on the flow due to rotating disk has been done by von Karman [5-6]. He was perhaps the first who derive a theoretical expression for the torque on a smooth disk rotating in an infinite fluid when the flow is turbulent. Early characterization of the hydrodynamics of a rotating disk in a closed cylindrical enclosure was reported by Daily and Nece in 1960 [7-10]. They showed that the hydrodynamic of a rotating disk with radius *r* and axial gap *s* in housing are governed by two parameters. Gap Reynolds number where the width of the gap is the characteristic length ($\mathrm{Re}_s = \omega \cdot s^2 / \upsilon$) or the radial Reynolds number where the radius of the disk is the characteristic ($\mathrm{Re}_r = \omega \cdot r^2 / \upsilon$), the second parameter is the ratio between the width of the gap and the disk radius (*s/r*). By measuring the torque acting on the shaft and correlating the frictional torque coefficient with the Reynolds number and axial clearance, they were able to differentiate four flow regimes. Region I: Laminar flow and narrow gap ($\sqrt{\mathrm{Re}_s} \le 4$, $\mathrm{Re}_r \le 2.10^5$), the boundary layers are merged and produce a shear rate varying inversely with spacing s. Region II: laminar flow and separate boundary layers ($\sqrt{\mathrm{Re}_s} \ge 4$, $\mathrm{Re}_r \le 2.10^5$), separate laminar boundary layers are formed and the shear rate is independent on *s*. between the two layers will develop a zone that moves like a solid body with a rotation–speed of *K*ω where 0 < *K* >1. Region III: Turbulent flow and narrow gap ($\mathrm{Re}_r \ge 2.10^5$ and *s/r* ≤ 0.05), the flow is characterised by merged turbulent boundary layers. Region IV: Turbulent flow and wide gap ($\mathrm{Re}_r \ge 2.10^5$ and *s/r* ≥ 0.05), two turbulent boundary layers with the angular velocity *K*ω, where 0 < *K* > 1.

There seems to be lack of computational works on estimating the skin friction for a porous disk rotating in a closed cylinder flow in axisymmetric laminar flow regime. Therefore, this paper aims to provide a CFD simulation study that focused on laminar flow regime and wide gap for a smooth porous disk rotating in a closed cylinder ($\mathrm{Re}_r \le 2.10^5$ and $\sqrt{\mathrm{Re}_s} \le 4$). Another sub goal of the present study is to test whether FLUENT, a commercial Computational Fluid Dynamics software package, is capable of providing the solutions for the problem under consideration.

2. THEORY

2.1. Governing equation

The steady laminar flow of viscous incompressible fluid and axisymmatric near an enclosed rotating disk with a constant angular velocity is considered. Under these conditions the incompressible Navier- Stokes equations in cylindrical polar coordinates reduce to.

$$v_r \frac{\partial v_r}{\partial r} - \frac{v_\theta^2}{r} + v_z \frac{\partial v_r}{\partial z} = -\frac{1}{\rho}\frac{\partial p}{\partial r} + \nu\left(\frac{\partial^2 v_r}{\partial r^2} + \frac{\partial}{\partial r}\left(\frac{v_r}{r}\right) + \frac{\partial^2 v_r}{\partial z^2}\right) \quad (1)$$

$$v_r \frac{\partial v_\theta}{\partial r} - \frac{v_\theta v_r}{r} + v_z \frac{\partial v_\theta}{\partial z} = +\nu\left(\frac{\partial^2 v_\theta}{\partial r^2} + \frac{\partial}{\partial r}\left(\frac{v_\theta}{r}\right) + \frac{\partial^2 v_\theta}{\partial z^2}\right) \quad (2)$$

$$v_r \frac{\partial v_z}{\partial r} + v_z \frac{\partial v_z}{\partial z} = -\frac{1}{\rho}\frac{\partial p}{\partial z} + \nu\left(\frac{\partial^2 v_z}{\partial r^2} + \frac{1}{r}\frac{\partial v_z}{\partial r} + \frac{\partial^2 v_r}{\partial z^2}\right) \quad (3)$$

$$\frac{\partial v_r}{\partial r} + \frac{v_r}{r} + \frac{\partial v_z}{\partial z} = 0 \quad (4)$$

where v_r , v_θ , v_z are the radial, tangential and axial components of the velocity, ρ is the fluid density and ν the

dynamic viscosity of the fluid. P denotes the fluid pressure.

2.2. *Boundary conditions*

Since the geometry of an axisymmetric geometry is considered a half geometry part rotated about an axis parallel to the velocity inlet is modeled. The bottom boundary of the domain is modeled as an axis boundary. The surface of the housing is modeled as a wall. The voids of the rotating filter disk is modeled as porous jump, where as the solid part as a wall. The exit of the permeable filter disk is modeled as pressure outlet. The flow inlet to the closed housing is modeled as velocity inlet.

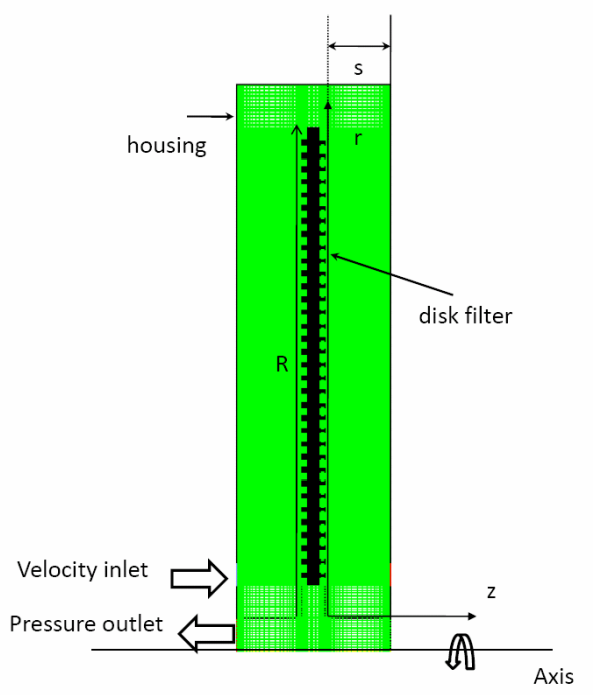

Figure-1. Schematic of the enclosed rotating disk filter showing the solution domain and Computational grid with boundary conditions.

2.2. Computational fluid dynamics

A finite volume method is employed using commercial software FLUENT 6.2 to solve the governing equations subject to specified boundary conditions. The model has been solved in two dimensions and the entire region is meshed (see Figure 1). The CFD tool can also accommodate numerous representation of flow in porous media. For a Newtonian isothermal and incompressible fluid, flow through a porous medium can be described using the porous jump model [8]. No slip boundary conditions are set at all solid wall boundaries. The flow inside the porous media is assumed to be laminar. More cells are constructed near the surface of the disk to compensate the high velocity gradient in the boundary layer region of the viscous flow. A commercial software GAMBIT is used for grid generation. The coupling between the pressure and velocity fields is achieved using PISO. A second order upwind scheme is used for the convection. Here in this study, the dimensionless torque coefficient (viscous drag coefficient) for a disk wetted on both sides and a Reynolds number can be defined as:

$$C_M = \frac{-2M}{1/2\,\rho\omega^2 r_o^5} \qquad M = \int_0^{r_o} \tau_{z\theta} r(2\pi r dr) \qquad \mathrm{Re}_r = \frac{\omega r_o^2}{\nu} \quad (5)$$

Where r_0 is the outer radius of the disk, M is the total torque required to turn a disk and $\tau_{z\theta}$ the tangential wall shear stress on the disk. The grid independence is achieved by comparing the results of the different grid cell size. It was found that 45000 cells are satisfactory, and any increase beyond this size would lead to an insignificant change in the resulting solution.

3. RESULTS AND DISCUSSIONS

CFD Simulation results for smooth rotating disk in closed housing are firstly compared to experimental data to verify the validity of the CFD simulation solution. Figure 2 shows the total viscous drag coefficient as a function of Reynolds number for the case of rotating disk. As can be seen from Figure 2, there is an excellent agreement in the Reynolds number dependence of C_M between CFD simulations in this study and the experimental measured dependence by [5]. The effects of Reynolds number on the total viscous drag coefficient for rotating filter and disk are shown in Figure 3. It is clear that C_M values gradually decrease with increase in Reynolds number for rotating filter and disk. It can also be seen that the rotating filter exhibit larger viscous drag coefficient compared to rotating disk due to the suction

effect on the boundary layers. This means, that more energy input is needed to turn the filter. The difference in the value of the viscous drag between the rotating filter and disk decrease significantly by increasing the Reynolds number especially at high Reynolds number. The reason behind that refers to the fluid flow turbulences. Figures 4 and Figure 5 show the axial distribution of swirl and radial velocities component respectively for rotating filter and disk. It is clear that for rotating filter the swirl velocity component decay sharply away from the filter surface. This in turns decrease the boundary layer thickness near the rotating filter surface and enhance the shear rate. The axial distribution radial velocity components close to the rotating filter surface increasing due to the effect of suction (see Figure 5).

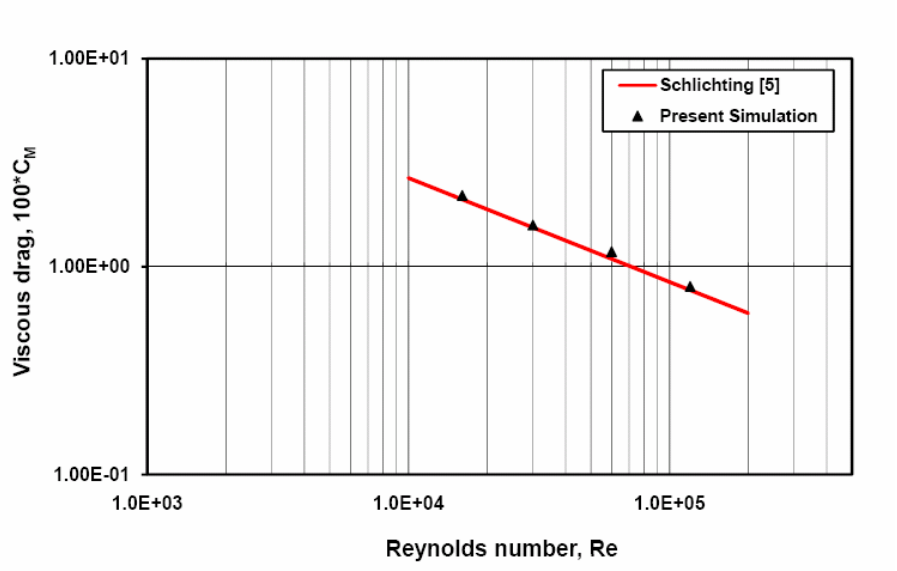

Figure-2. Comparison of computed viscous drag of disk rotating in a housing with the experimental correlation Schlichting [5].

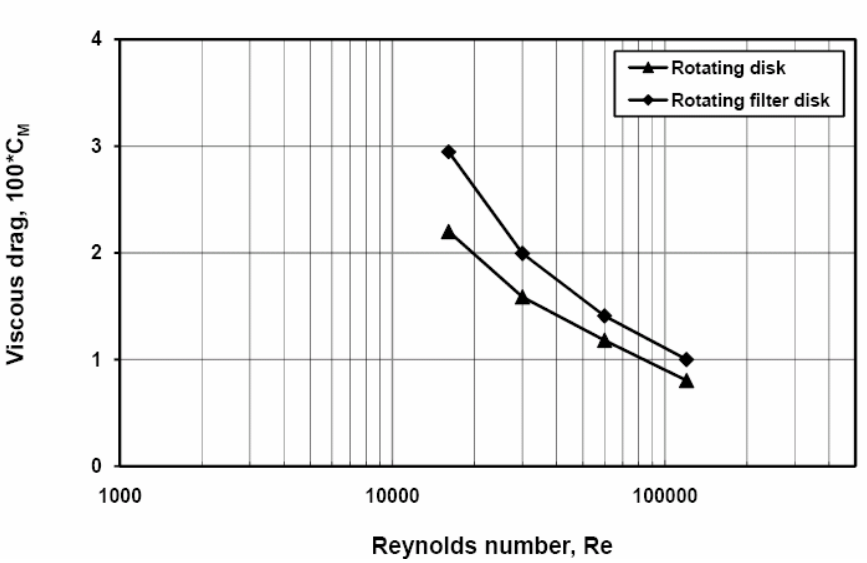

Figure-3. Variation of the viscous drag as a function of Reynolds number for rotating filter and disk.

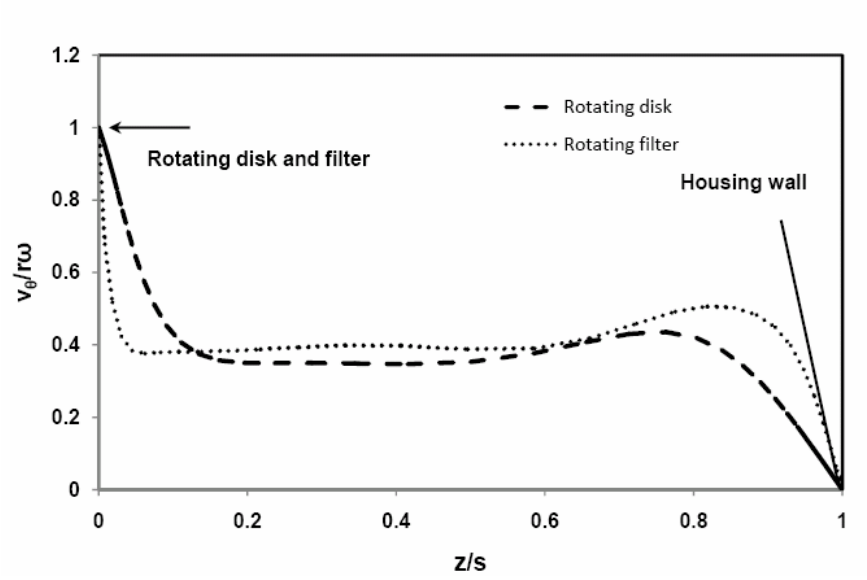

Figure-4. The axial distribution of swirl velocity for rotating filter and disk at a radial distance $r/R = 0.5$ for $Re_r = 2.3\times10^4$

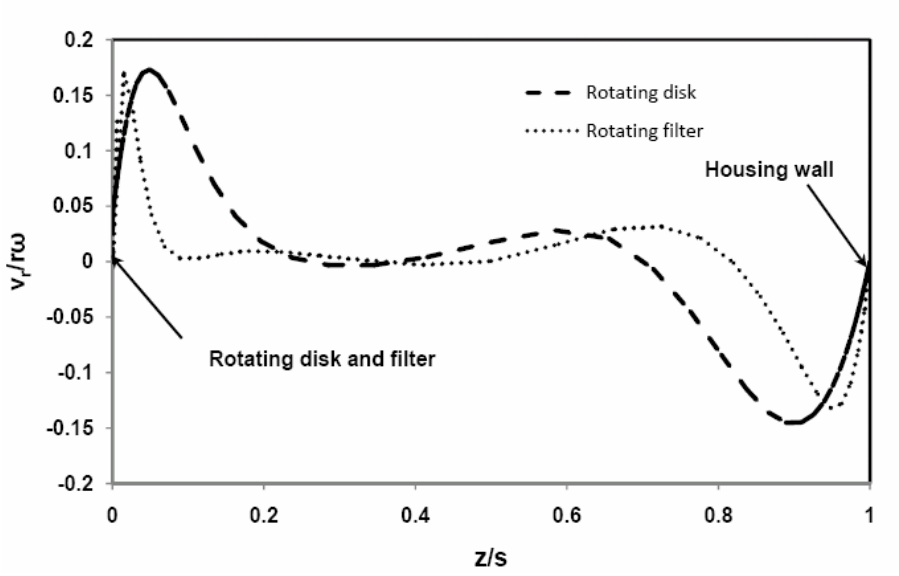

Figure-5. The axial distribution of radial velocity for rotating filter and disk at a radial distance $r/R = 0.5$ for $Re_r = 2.3\times10^4$

The effect of filter rotation on the flow pattern is illustrated clearly on streamline contour Figure 6 (a).

The rotation speed of the filter disk leads to fluid circulation. Figure 6 (b) shows the contours of static pressure for rotating filter in closed housing. It can be seen that the local pressure surrounding the rotating filter is almost constant. Whereas, the static pressure inside the filter varies according to the centrifugal force induced inside. Since the centrifugal force depends only on the rotation speed of the filter and not on the local pressure inside the housing, we expect that by increasing the rotation speed of the filter a back pressure is produced and thus low permeate rate is obtained.

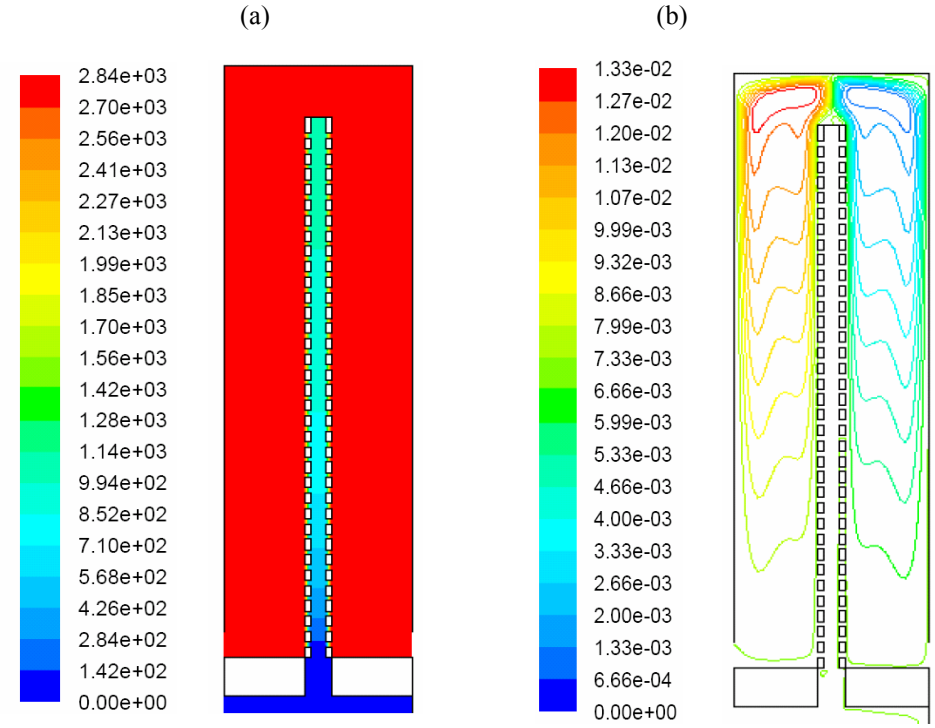

Figure-6. (a) Contours of static pressure in Pa (b) variation of contours of stream function for rotating disk at $Re_r = 2.3\times10^4$

4. CONCLUSIONS

The steady laminar flow of viscous incompressible fluid induced by a smooth rotating filter and disk in closed housing using computational fluid dynamics are carried out. The nature of the fluid flow near a rotating disk and filter inside a closed housing was visualised. The dependency of the viscous drag coefficient on the Reynolds number was shown. It was found that the rotating filter exhibit larger viscous drag coefficient due to the suction effect on the boundary layers. A high rotation speed of filter may produced a back pressure which could be reduced by increasing the inlet feed pressure. Comparison the simulation results with the experimental data validate the commercially-available software FLUENT in providing a reasonable good solution of complicated flow structures, including flow with circulation. It remains to be verified the effect of filter permeability, feed pressure, angular velocity of the filter on the rotating filter performance. Such simulation are currently under way and results will be reported in forthcoming manuscript

REFERENCES

[1] Daily JW, Nece RE. 1960. Chamber dimension effects on induced flow and frictional resistance of enclosed rotating disks. J. Basic Eng. 82: 648-653.

[2] J. Mukes and C.G. Carlsson. 1988. Crossflow Filtration. Wiley, New York.

[3] Y. Taamneh. 2009. Numerical and Experimental Investigation of Dynamic Filters. PhD Thesis. TU Kaiserslautern, Germany.

[4] R. Boozerare, M. Y. Jaffrin, L. Dingand P. Paullier. 2000. Influence of geometry and angular velocity on performance of a rotating disk filter. AICHE j. 46: 257-265.

[5] Schlichting H. Boundary layer Theory, New York: McGraw-Hill; 1969.

[6] J.A. Engler. 1997. Investigation of membrane filtration in a rotating disc geometry: using of computational fluid dynamics and laboratory evaluation. PhD thesis. Rice University, Houston.

[7] C. A. Serra, M. R. Wiesner. 2000. A comparison of rotating and stationary membrane disk filters using computational fluid dynamics. J. Membr. Sci. 165: 19-29.

[8] Y. Taamneh, S. Ripperger. 2010. Approximate Solution Using Momentum Integral in Estimating the Shear Stress over a Porous Rotating Disk. International Journal of Dynamic of Fluids. 6(5) : 215-222.

[9] Y. Taamneh, S. Ripperger. 2008. Performance of single and double shaft disk separator. Physical Separation in Science and Engineering. 2008 (1): 1-5

[10] Y. Taamneh, L. Steinke, S. Ripperger. 2008. Investigation of Dynamic Filters Using CFD. 10th World Filtration Congress Proceedings. 2: 472-476.

[11] Y. Taamneh, L. Steinke and S. Ripperger. 2007. Einfluss der Geometrieverhältnisse auf die Separation mittels rotierender Membranen. Chemie Ingenieur Technik. 79(9): 1475-1475.